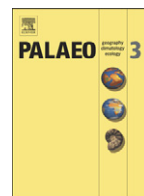




Contents lists available at ScienceDirect

Palaeogeography, Palaeoclimatology, Palaeoecology

journal homepage: www.elsevier.com/locate/palaeo

Quantifying climate change in Huelmo mire (Chile, Northwestern Patagonia) during the Last Glacial Termination using a newly developed chironomid-based temperature model

Julietta Massafiero^{a,*}, Isabelle Larocque-Tobler^b, Stephen J. Brooks^c, Marcus Vandergoes^d, Ann Dieffenbacher-Krall^e, Patricio Moreno^{f,g}

^a CENAC/APN, Fagnano 244, 8400 Bariloche, Argentina

^b The L.A.K.E.S. Institute, Dreihubelweg 68, 3250 Lyss, Switzerland

^c Department of Life Sciences, Natural History Museum, Cromwell Road, London SW7 5BD, UK

^d GNS Science, Lower Hutt 5040, New Zealand

^e School of Biology and Ecology, University of Maine, Orono, ME 04468, USA

^f Institute of Ecology and Biodiversity, Universidad de Chile, Santiago, Chile

^g Department of Ecological Sciences, Universidad de Chile, Santiago, Chile

ARTICLE INFO

Article history:

Received 30 August 2013

Received in revised form 13 January 2014

Accepted 18 January 2014

Available online xxx

Keywords:

Chironomids

Temperature reconstruction

Younger Dryas

Huelmo–Mascardi Cold Reversal

Antarctic Cold Reversal

Northern Patagonia

ABSTRACT

The development of quantitative temperature reconstructions in regions of paleoclimate interest is an important step for providing reliable temperature estimates in that region. Fossil chironomid assemblages have been studied in Patagonia showing great promise for reconstructing paleotemperatures; however there is still a lack of robust temperature inference models in that area.

To contribute to the understanding of climate change, a transfer function using chironomids preserved in 46 lakes in Chile and Argentina was developed. The best performing model to infer the mean air temperature of the warmest month was a 3-component WA-PLS model with a coefficient of correlation (r^2_{jack}) of 0.56, a root mean square error of prediction (RMSEP) of 1.69 °C and a maximum bias of 2.07 °C. This model was applied to the chironomids preserved in the sediment of the Huelmo mire (41°31' S, 73°00' W), in the lake district of north-western Patagonia. The reconstruction showed several cold spells (one at 13,200 to 13,000 cal yr BP and a cooling trend between 12,600 and 11,500 cal yr BP) associated with the Younger Dryas and/or Huelmo–Mascardi Cold Reversal (HMCR). Our findings support climate models proposing fast acting inter-hemispheric coupling mechanisms including the recently proposed bipolar atmospheric and/or bipolar ocean teleconnections rather than a bipolar see-saw model.

© 2014 Elsevier B.V. All rights reserved.

1. Introduction

Patagonia is an important area for paleoclimate studies in southern South America because it is significant in understanding climate synchronization between the North and South Hemispheres. However, views are still polarized concerning climate dynamics during key periods of large-scale climate fluctuations (e.g. the Lateglacial/Holocene transition) (Whitlock et al., 2006; Rojas et al., 2009; Killian and Lamy, 2012). Despite efforts to identify climate fluctuations after the Last Glacial Maximum (LGM), the timing and extent of a cold reversal contemporaneous to the Younger Dryas (YD) is still in unresolved. Divergent evidence comes from paleoclimate studies based mainly on terrestrial records from the Andean Patagonian forest of Chile and Argentina. These studies show either i) a cooling pattern synchronous

with the YD (12,500 to 11,200 cal yr BP) (Heusser et al., 1996; Ariztegui et al., 1997; Moreno, 1997, 2004; Moreno et al., 2001; Massafiero and Brooks, 2002); ii) a cooling pattern synchronous with the Antarctic Cold Reversal (ACR, 14,500 to 13,000 cal yr BP) (Lamy et al., 2004; Moreno et al., 2009); or iii) an intermediate YD/ACR climate signal called Huelmo–Mascardi Cold Reversal (HMCR, 13,500 to 11,600 cal yr BP) (Hajdas et al., 2003; Bertrand et al., 2008b; Massafiero et al., 2009). Differences between these records may be attributed to the individual response of proxies, chronological control, sampling resolution, individual site characteristics, the differential influence of the Southern Westerly Winds (SWW) on the east or west side of the Andes or merely because the signature of the cold event in the southern hemisphere is weak. In New Zealand, similar discrepancies were apparent during the Late Glacial/Holocene transition (Denton and Hendy, 1994; Newnham et al., 2003; Turney et al., 2003; McGlone et al., 2004). Resolving this problem is important for understanding the intra- and inter-hemispheric modes of millennial-scale climate changes during the Last Glacial Termination, and for determining the

* Corresponding author. Tel.: +54 294 4433522.

E-mail address: julimassafiero@hotmail.com (J. Massafiero).

URL: <http://www.cenacbariloche.com.ar> (J. Massafiero).

climatic mechanisms involved in their initiation and propagation. Production of quantitative, high resolution reconstructions of summer temperature will be particularly important in this respect. To contribute to the resolution of this problem we have used chironomids to obtain a summer temperature reconstruction, the first of its kind in northern Patagonia, from a Late Glacial lake sediment sequence.

Summer temperature is one of the major controls over the chironomid life cycle (Rossaro, 1991; Brodersen and Lindegaard, 1999) and many models (transfer functions) have been developed in the Northern Hemisphere to quantify summer temperature (e.g. Walker et al., 1991; Olander et al., 1999; Brooks and Birks, 2001; Larocque et al., 2001, 2006; Self et al., 2011; Eggermont and Heiri, 2012). In the southern Hemisphere, transfer functions have been developed for southern Patagonia (Massafiero and Larocque, 2013), northern Chile (Araneda et al., in prep), Tasmania (Rees et al., 2008) and New Zealand (Dieffenbacher-Krall et al., 2007; Woodward and Shulmeister, 2007) showing the potential of using chironomids in this region for temperature reconstruction. Even though northern Patagonian paleoenvironmental investigations using chironomids are not numerous, there are several qualitative and semiquantitative records indicating that changes have occurred in this faunal community during the Late Glacial period (Massafiero and Brooks, 2002; Massafiero et al., 2009). A recent quantitative reconstruction at Potrok Aike, in southern Patagonia, confirms the potential of chironomids to help in understanding the complex climate fluctuations in southern South America (Massafiero and Larocque, 2013).

In this paper, we present the first quantitative chironomid-inferred temperature model for Northern Patagonia (Argentina and Chile) and use it to reconstruct temperatures during the Late Glacial from a fossil chironomid record from Huelmo mire, located in Chilean Patagonia at 41° S. An earlier qualitative analysis of chironomids and pollen from Huelmo indicated temperature and precipitation changes between ca. 20 and 10 cal kyr BP (Massafiero et al., 2009). The chironomid and pollen records from Huelmo indicated step-wise deglacial warming beginning at ca. 18,000 cal yr BP, in agreement with other paleoclimate records from northwestern Patagonia, and ice core records from Antarctica (Pedro et al., 2011). Isotopic signals from Antarctic ice cores indicate relatively warm conditions between ~15,000 and 14,000 cal yr BP, followed by a reversal in trend with cooling pulses at ~14,000 and 13,500 cal yr BP, and warming at the beginning of the Holocene (Jouzel et al., 2003). Peak warmth during the Last Glacial Termination was achieved during ~14,500 cal yr BP, followed by a cooling trend that commenced during the ACR (~14,000 cal yr BP), which later intensified and persisted during the so-called Huelmo–Mascardi Cold Reversal (HMCR) (Hajdas et al., 2003; Massafiero et al., 2009). A reconstruction of temperature using chironomids will quantify the warmer and colder periods suggested by the previous pollen and chironomid records.

2. Site location

The Huelmo mire (41°31' S, 73°00' W) is located in the lowlands of the southern Chilean Lake District, on the western side of Seno Reloncaví (Fig. 1). The area is characterized by a mix of Valdivian, North Patagonian and temperate rainforest vegetation. The area that surrounds Huelmo has been altered by human activities. Current vegetation close to the mire is heavily influenced by clearance, leaving grassland for grazing. Quaternary glacial, volcanic, eolian and alluvial–colluvial deposits cover most of the bedrock geology in the area (Heusser, 1999).

At Puerto Mont, on the northern shore of Seno Reloncaví, mean annual temperature is 11.2 °C (ranging from 7.7 °C in winter to 15.1 °C in summer) and mean annual precipitation is 2341 mm (Moreno and Leon, 2003). This cool-temperate, wet climate results from the cold, offshore Humboldt Current combined with the Southern Westerly Winds (SWW) (Garreaud et al., 2009).

3. Material and methods

3.1. Sampling, stratigraphy and chronology

Several overlapping sediment cores from the center of the Huelmo mire were extracted using a square-rod Livingstone corer. For this study, cores 601A, 990-1A and 990-1B were combined in a 421 cm long composite sequence spanning the time interval between 19,600 and 10,000 cal yr BP (1071–650 cm). Stratigraphic correlation between these cores was achieved using loss-on-ignition records and two prominent tephra layers (Moreno and Leon, 2003). The stratigraphy of the composite core consisted of a floor of sand and gravel grading to silt with increasing amounts of organic material. On top of this, there was a sequence of organic gyttja, a thick sand volcanic ash layer, coarse organic detritus with gyttja and woody peat on top. The chronology of the core was based on 37 AMS radiocarbon dates, which were converted to calendar yr BP using CALIB 4.1.2 (Stuiver et al., 2005). The age–depth curve reveals continuous sedimentation along the time span of the composite core (Fig. 2). More details about lithology and age model are discussed in Moreno and Leon (2003).

The core stratigraphy together with the age–depth curves, X-radiographs and loss-on-ignition data indicate a major change in depositional patterns above and below a prominent volcanic ash at 696 cm depth (interpolated age of 11,000 cal yr BP). Before this ash layer, pelagic sedimentation prevailed indicating the presence of a permanent lake. After the tephra deposition, the Huelmo site underwent a rapid drop in lake-level and the expansion of a swamp (indicated by a shift to coarse detritus gyttja/woody peat) (Moreno and Leon, 2003).

3.2. Training set lakes

Thirty lakes were sampled during the austral summer of 2000 and 2002, six of them are located in Chile and twenty-four in Argentina, along an altitudinal gradient of 72.4 to 1925 m a.s.l., between 39° to 43° S and 70° to 73° W (Table 1). An additional 16 lakes from Argentina were incorporated into the training set in 2007 in order to increase the temperature gradient. Each lake was sampled using a mini-Renberg gravity corer (the first 30 lakes) or a Hongve-style gravity corer (the remaining 16 lakes) to preserve the sediment–water interface and the top 2–3 cm of the sediment was taken. Ninety percent of the sampled sites were located in areas with minimal human disturbance, such as national parks and nature reserves. Most of the high altitudinal lakes were located above the treeline in remote and pristine areas of Argentina. The environment encircling the lakes was similar on both sides of the Andes. Northern Patagonia is a lake district in both Argentina and Chile and the vegetation is composed of a mix of Valdivian, evergreen and temperate forest elements.

A range of environmental variables (secchi depth, conductivity, surface temperature, total dissolved solids and pH) were measured for each lake. Mean annual air temperature (MAT), mean annual precipitation (MAP), mean temperature of the three warmest months (WMM) and mean temperature of the three coldest months (CMM) were obtained from the BRIDGE gridded data (New et al., 2002). Altitude and depth were also included in the training set. The surface water temperature gradient was 6.0–20.5 °C and mean summer air temperature ranged from 8.9 to 17.5 °C. The pH varied from 4.0 to 8.4 and conductivity from 0.14 to 126 µS.

All of the studied lakes are oligotrophic or hyperoligotrophic (Balseiro et al., 2004; Callieri et al., 2007; Diaz et al., 2007); thus nutrient content, phosphorus and chlorophyll a are below detection levels. As these systems are nutrient-poor, most are expected to be oxygen-rich, thus oxygen is not likely to be significant in explaining the distribution and abundance of chironomids in these lakes.

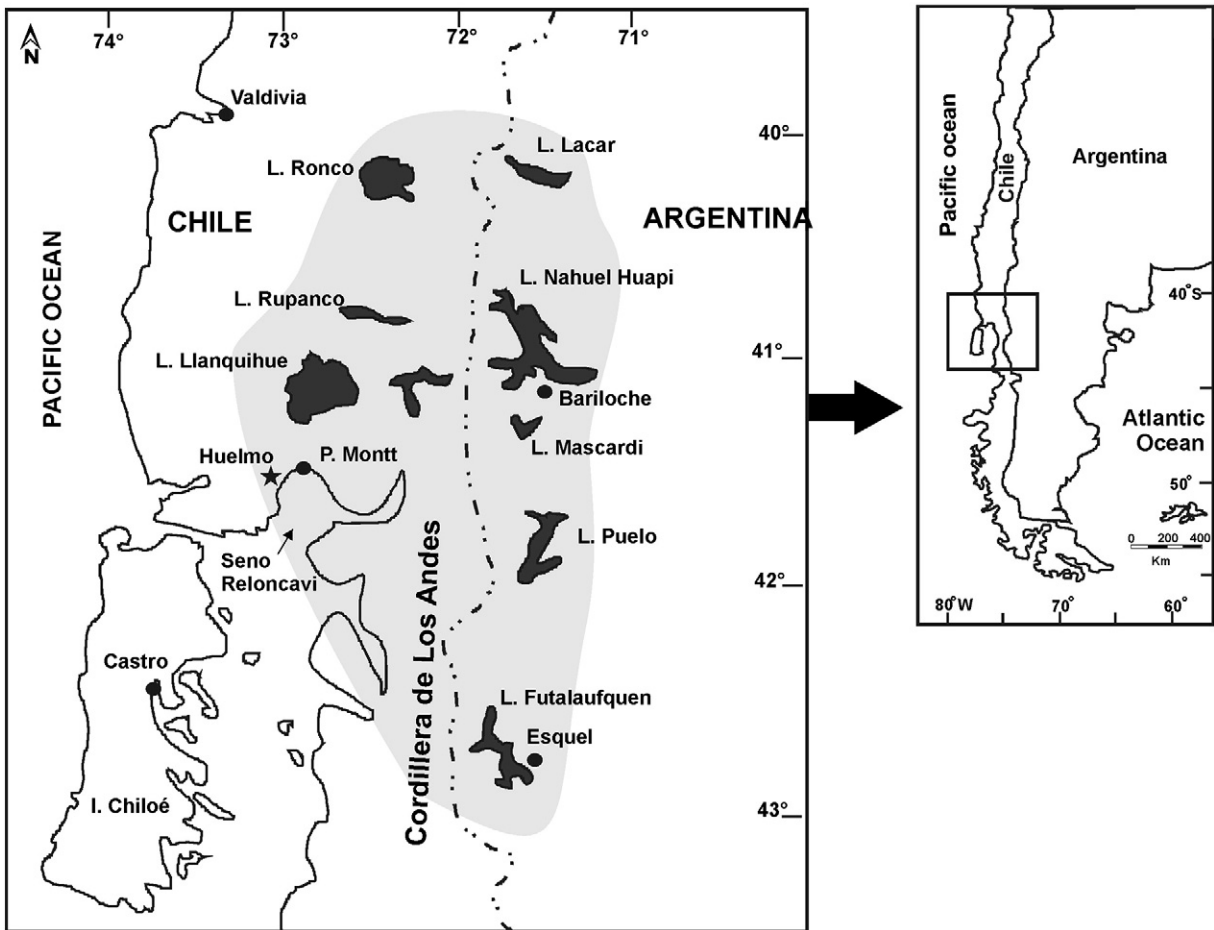


Fig. 1. Location map of training set lakes (gray shadow area) and Huelmo mire (black star).

3.3. Chironomid analysis

Following Walker et al. (1991), 5 to 10 g of sediment was examined for chironomid head capsules. Sediment was deflocculated using 10% KOH and sieved through 100 and 200 μm mesh size. The material

retained by the meshes was hand-sorted in a modified Bogorov counting tray under a dissecting microscope at 20 \times magnification. Individual head capsules were placed on microscope slides in a drop of Hydro-Matrix®. Identification was made using a Nikon Phase microscope at 400 \times magnification. Head capsules were identified with

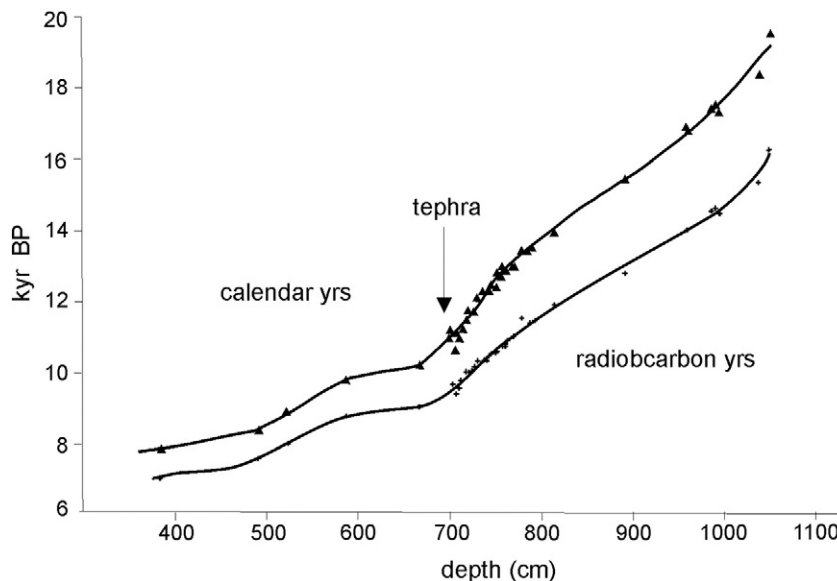


Fig. 2. Age versus depth curve of composite Huelmo core 901B-601A showing the age models applied to the uncalibrated and calibrated radiocarbon dates obtained by CALIB 4.1.2.

Table 1

Lakes and environmental variables included in this study. Last column shows the total number of chironomid head capsules (HC).

ID	Lake	Long (W) (dec)	Lat (S) (dec)	Altitude (m a.s.l.)	Depth (m)	Secchi (m)	pH	Cond ($\mu\text{g/l}$)	Temp top ($^{\circ}\text{C}$)	Air temp ($^{\circ}\text{C}$)	MAT ($^{\circ}\text{C}$)	WMM ($^{\circ}\text{C}$)	CMM ($^{\circ}\text{C}$)	MAP (mm)	Total nr HC
1	Pire	71.80722	40.78889	738	20	6.2	5.93	36.4	16.1	16.17	9.27	15.08	4.02	125.13	41
2	Bailey Willis	71.705	40.7	799	8.9	2.8	4.05	0.14	20.5	16.17	9.19	15.12	3.82	122.23	108
3	Trebol	71.44111	41.16389	760	10.5	3.8	7.75	92.4	18.3	16.17	9.03	14.97	3.48	91.86	182
4	Escondido	71.44111	41.16389	754	7.2	5.18	7.53	63.8	19.3	16.17	9.06	15.01	3.51	91.86	125
5	Morenito	71.52139	41.13611	754	8.5	4.8	7.67	78	18.6	16.17	9	14.88	3.55	96.02	218
6	Verde	71.71722	40.69444	1466	1.5	0.92	7.48	34.1	15.5	11.84	5.39	11.21	0.091	123.24	102
7	Fon	71.29861	41.35556	750	17.5	6.1	7.66	7.66	17.6	16.17	9.19	15.24	3.45	81.49	75
8	Hess	70.73639	41.37222	730	8.3	8.3	7.39	45.9	17.7	16.17	9.6	16.11	3.32	54.34	173
9	Moscós	71.61806	41.49444	803	20	7.6	7.56	53.7	18.4	15.26	8.44	14.26	2.97	97.85	142
10	Gallinas	71.61806	41.49722	998	8.5	6	7.02	32	13.3	14.69	7.33	13.13	1.86	97.83	152
11	Patos	71.00361	40.76111	973	7.2	5.1	6.97	33.1	16.1	14.69	8.42	14.88	2.4	81.16	132
12	Angostura	71.65917	40.86389	768	5.5	2	7.55	17.5	19.4	16.17	9.19	15.11	3.8	113.96	153
13	Huala Hue	71.50917	41.64444	828	6.7	6.7	8.85	126.6	14.3	15.26	9.15	15.28	3.6	110.47	157
14	Lezama	71.46306	42.49722	679	7	7	8.48	103.6	19.1	16.4	8.8	14.69	2.88	83.26	93
15	Redonda	71.5625	40.98889	840	7.6	1.9	7.04	63.3	16.4	15.26	8.7	14.64	3.23	104.37	213
16	Mercedes	71.57306	41.00278	818	20	5.2	7.29	48.9	18.3	15.26	8.66	14.48	3.3	99.7	93
17	Larga 1	71.57	40.04082	830	17	5.5	7.42	48.8	17.4	15.26	9.8	16.02	4.31	118.27	77
18	Futaleufu	71.86	43.18611	324	10	4.7	7.52	50.3	16.2	17.55	11.9	17.26	6.37	128.16	93
19	Leta	73.16472	41.57778	72.4	2.5	2.05	6.01	19.7	19	14.38	10.14	14.38	6.53	165.11	288
20	Blanco 2	72.60667	42.75278	98	29	4.82	6.73	18.1	14.2	14.38	10.37	15.11	5.75	174.79	91
21	Tamango	71.90194	43.34444	415	5	4.4	6.91	53.5	12.6	12.1	11	16.3	5.51	130.11	266
22	Maniguales	72.14639	43.3	130	19.5	3.6	6.84	12.88	15	16.03	11.69	16.76	6.5	148.58	149
23	clubandino	71.628	41.153	1600	10	8	7	8.8	10.2	10.7	4.07	9.78	-1.23	100.95	15
24	Mallin ricardo	71.715	41.18	1571	5	3	6.4	56	11	11.27	4.14	9.79	-1.08	104.99	23
25	Alerzales	71.671	41.713	1374	5	1	6.5	28	11	12.41	4.97	10.76	-0.53	99.55	30
26	Mellizas	71.342	40.621	1067	16	4	8.02	112	13	14.69	7.84	14.1	2.17	99.38	24
27	Cuyen	71.761	41.522	1715	11	11	7	13	11.4	10.13	2.97	8.7	-2.39	106.15	5
28	Campana	71.828	40.6	1250	9	7	7.3	7	8.8	13.55	6.55	12.32	1.36	132.26	5
29	Aguirre	71.82	41.477	1418	8	8	7	9	9	11.84	6.5	11.66	1.49	165.12	20
30	Ilon	71.73	41.19	1359	26	15	7.4	17.5	11	12.98	5.33	10.99	0.11	105.69	8
31	Jujuy	71.695	41.191	1838	6	6	7.5	9	9.6	9.56	2.63	8.27	-2.6	103.96	6
32	Azul	71.68	41.208	1509	18	15	7.1	5	10	11.27	4.51	10.2	-0.76	103.13	30
33	Creton	71.671	41.194	1648	9	7	7.04	6	12	10.7	3.74	9.41	-1.54	102.77	24
34	Matedulce	71.673	41.165	1635	7	6	6	5	8.6	10.7	3.83	9.5	-1.43	103.04	23
35	Lafea	71.641	40.826	1149	21	3	7.7	77	11.2	14.12	7.07	12.96	1.69	114	3
36	Negra	71.34	41.13	1617	21	18	7.94	8	11	10.7	4.24	10.17	-1.37	87.57	55
37	Plato	71.552	39.567	1341	12	6	8.2	43	9	12.98	6.64	12.82	1.05	115.23	84
38	Schmol	71.497	41.193	1925	8	8	7.16	10	6	8.99	2.32	8.11	-3.12	94.22	86
39	Jacob	71.559	41.186	1572	25	16	7.45	16	9	11.27	4.28	10.05	-1.11	97.33	67
40	Toncek	71.486	41.198	1747	12	6	8.16	12	8	10.13	3.34	9.16	-2.12	93.62	60
41	Quillehue	71.517	39.562	1118	55	4	8.3	33	8	13.55	8.03	14.31	2.35	113.4	15
42	Vadeo	71.823	41.056	1303	7	2	7.66	45	6	12.98	5.48	11.05	0.39	111.77	83
43	Los Clavos	71.825	41.046	1194	27	7	7.23	54	7	13.55	6.1	11.68	1.01	111.94	26
44	Rosada	71.814	41.248	1372	24	5	8.4	11	8	12.98	5.01	10.62	-0.15	110.52	74
45	Tempanos	71.063	41.185	1660	11	11	6.87	6	6	10.7	4.04	10.21	-1.84	72.83	32
46	Juventus	71.528	41.358	1004	37	8	7.66	85	11	15.26	7.47	13.34	1.97	93.98	80
47	Guillermo	71.5	41.35	980	130	8	7.47	57	10	15.26	7.65	13.53	2.11	92.54	44

reference to available taxonomic literature (Wiederholm, 1983; Cranston, 2000) and a Patagonian subfossil chironomid taxonomic identification guide (Massaferrero et al., 2013).

3.4. Statistical analysis

For all statistical analyses, only the taxa with percentages higher than 3% in at least one lake were retained. Environmental data were log transformed and chironomid percentage values were squared root transformed to stabilize variances. Detrended Correspondence Analysis (DCA, Hill and Gauch, 1980), with detrending by segments and non-linear rescaling of axes, was used to explore the main patterns of taxonomic variation among sites and to estimate the compositional gradient lengths along the first four DCA axes. Because the gradient length of axis 1 was larger than 2 standard deviation units, unimodal techniques were used to explore the importance of the environmental factors on the distribution of the taxa with a Canonical Correspondence Analysis (CCA) (Birks, 1998). The forward selection option of CCA was used to identify a subset of the environmental variables that each explained significant variation in the chironomid data. Statistical significance of

each forward-selected variable was tested by a Monte Carlo permutation test (999 unrestricted permutations) (ter Braak, 1990; ter Braak and Verdonschot, 1995), using a Bonferroni-type adjustment for significance levels as described by Lotter et al. (1997). We further assessed the strength of relationships between chironomids and each of the forward-selected variables using constrained and partial CCAs (Rosén et al., 2000). Variance partitioning (Borcard et al., 1992) was used to explain the independent explanatory power of each forward selected variable. Finally, a DCCA was used to determine how much each of the selected variables individually explained the variation in the distribution and abundance of chironomids in the 46 training set lakes. The ratio of λ_1/λ_2 (i.e., ratio of eigenvalues of the first constrained DCCA axis 1 and the second unconstrained DCA axis 2) was used to provide a measure of the predictive power of the inference model. All ordinations were performed using the computer program CANOCO version 4.0 (ter Braak and Smilauer, 1998) with chironomid percentages square root transformed and rare taxa down-weighted.

Because the data showed unimodality, quantitative transfer functions would be developed using weighted-averaging regression and calibration partial least squares (WA-PLS; ter Braak and Juggins,

1993). The optimal number of components to include in the transfer functions was assessed by jack-knifing (ter Braak and Juggins, 1993). The models were developed using the program C2 (Juggins, 2007).

4. Results

4.1. Exploratory analysis

After removing the taxa present in only one lake at percentages lower than 3%, 49 taxa were retained in the dataset of 46 sampled lakes. The length of the first DCA gradient was 3.872, suggesting a unimodal distribution of taxa. WMM, secchi depth and conductivity were the three variables with the highest and significant scores of variability explained. The first significant axis of the CCA explained 36.3% of the variance while CCA axis 2 explained only 12.8% of the variance (Fig. 3). Alone, WMM explained 22.44% of the variance, secchi depth explained 10.3% of the variance and conductivity explained 9.31% of the variance. Variance partitioning indicated that WMM accounts for a significant ($p \leq 0.05$) independent fraction of 18% of the variance in the chironomid data and only a very small fraction (4%) is the shared effect with the two other variables, conductivity and secchi depth. WMM had the highest DCCA λ_1 /DCCA λ_2 ratio (1.735) and was used to develop a transfer function.

4.2. Distribution of taxa in the training set lakes

Ablabesmyia was the most common taxon (32 lakes) followed by *Tanytarsini 1A* (27 lakes), *Apsectrotanypus* (26 lakes), *Cricotopus* (25 lakes), *Chironomus* (25 lakes), *Parapsectrocladius* (24 lakes), *Tanytarsini 1B* (24 lakes) and *Tanytarsini D* (23 lakes). *Smittia* was found at highest percentages in cold (8–10 °C) lakes and, sporadically, at lower percentages in lakes up to 12 °C (Fig. 4). *Riethia* appeared at high percentages (up to 80%) in lakes between 10 and 12 °C and decreased to about 20% in lakes between 12 and 16 °C. *Phaenopsectra* was present in low percentages in lakes between 10 and 12 °C and had its highest percentage (50%) in one lake at ca. 15 °C. *Lauterborniella*, *Paracladius*, *Procladius*, *Tanytarsini B2*, *Gymnometriocnemus*, *Labrundinia*, *Orthocladiinae type3*, *Parachironomus*, *Corynoneura*, *Tanytarsini B*, *Nanocladius*, *Parachironomus*, *Rheotanytarsus* and *Pentaneurini* appeared only in lakes warmer than 12 °C. All of these taxa have their maximum percentages between 14 and 15 °C.

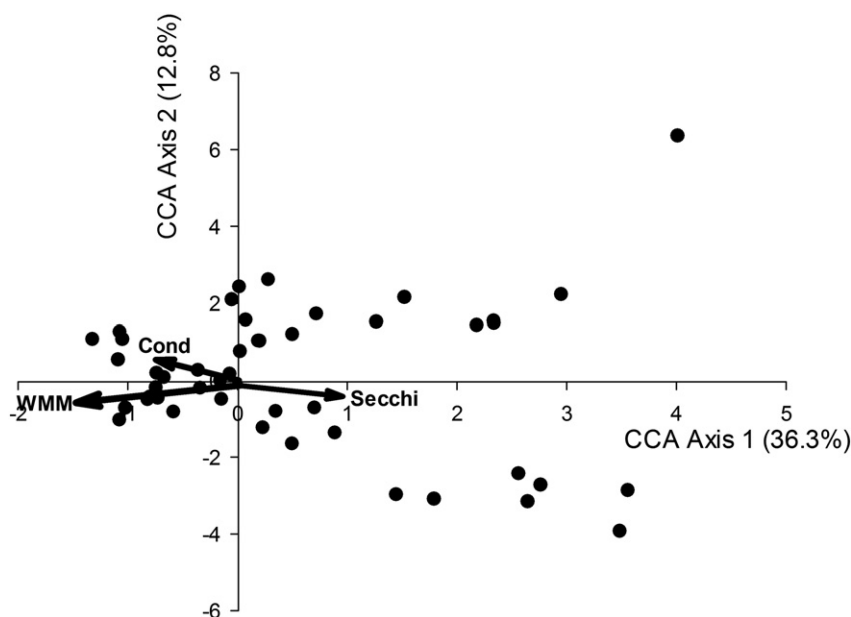


Fig. 3. Canonical Correspondence Analysis (CCA) of the training set lakes. The arrows represent the three variables explaining the best the chironomid distribution in these lakes. WMM = warmest months mean, Cond = Conductivity and Secchi = Secchi Depth.

4.3. Development of the transfer function

The development of the transfer function was restricted by the low number of chironomids found in many of the lakes. For adequate development of models, it has been shown that the highest number of lakes and taxa usually increases the performance (i.e. highest correlation coefficient, r^2) (Larocque et al., 2009). However, this consideration is made when at least 50 head capsules (hc) per sample are used for reconstruction (Heiri and Lotter, 2001; Larocque et al., 2001; Quinlan and Smol, 2001a). In hyper-oligotrophic lakes and in lakes with low organic content finding 50 head capsules per sample are not practical (Massafarro and Vandergoes, 2013). In this study, more than 10 g of sediment was processed in most lakes, but this high amount often did not yield 50 or more head capsules, especially in hyper-oligotrophic lakes located above the treeline (see Table 1). Thus, we compared the results of three different models: 1) using all lakes, 2) removing lakes with less than 30 hc and 3) removing lakes with less than 15 hc. The statistical performances of these models are given in Table 2. The best model was the WAPLS with 2 components including lakes with at least 15 hc ($r^2_{\text{jack}} = 0.56$, $\text{RMSEP}_{\text{jack}} = 1.69$; $\text{Max Bias}_{\text{jack}} = 2.07$). Both this model (>15 hc) and the model using only lakes with more than 30 hc do not have the lakes evenly distributed along the temperature gradient: there is no lake at 11.5 °C in the model with >15 hc, while no lake around 12 °C is present in the model with >30 hc. The model with >30 hc underestimated the coldest lake (5 °C instead of 9 °C) but the other lakes are closer to the 1:1 line (Fig. 5). One lake was overestimated by 5 °C in the >15 hc model, but all other residuals were between +2 and -4, while in the model with all lakes, many residuals were around +4 and -3.

4.4. Chironomids at Huelmo

Fifty-eight taxa were found in the 105 sediment samples of Huelmo (Massafarro et al., 2009). *Tanytarsini 1A* was found in 99 of the samples, and taxa found in more than half of the samples were *Tanytarsini 1B*, *Riethia*, *Chironomus*, *Tanytarsini 1D*, *Apsectrocladius*, *Tanytarsini 1C*, *Polypedilum*, *Ablabesmyia*, *Parachironomus* and *Labrundinia*. The zones in the stratigraphy were created by the expected timing of the ACR (14,500 to 13,000 cal yr BP) and the YD (12,500 to 11,200 cal yr BP) in this region (Fig. 6). Before the ACR (19,000 to 14,500 cal yr BP), the

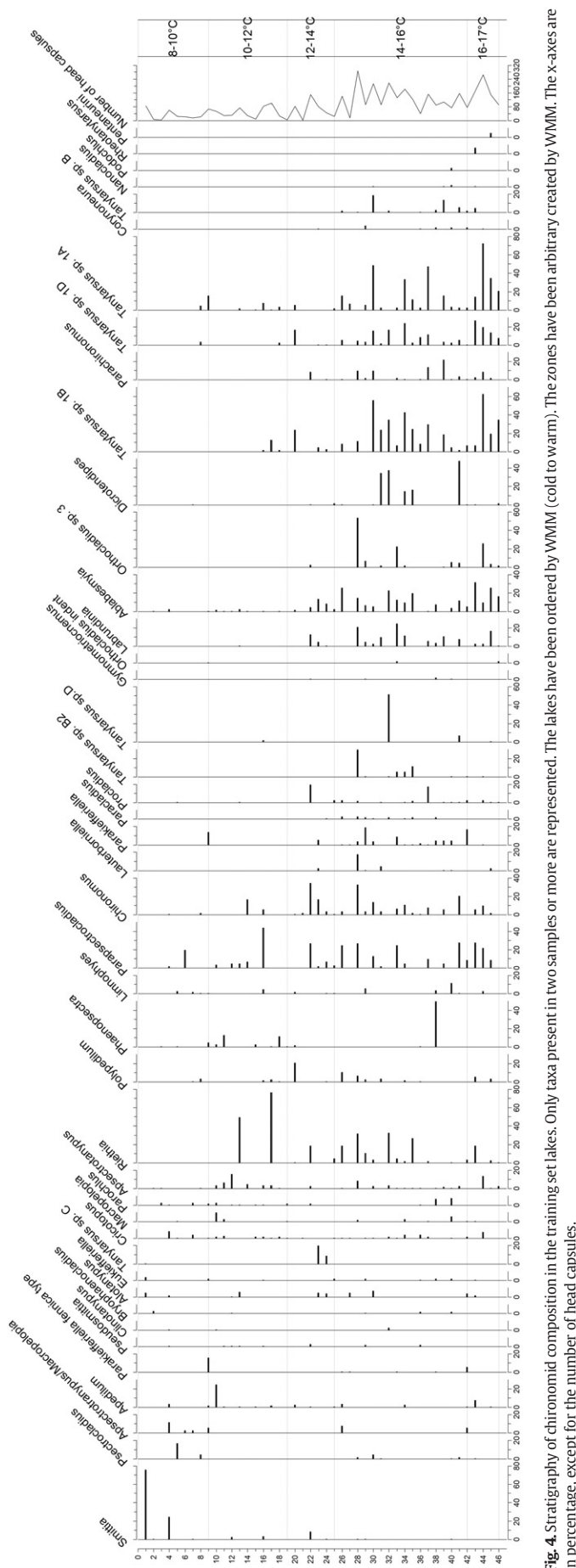


Fig. 4. Stratigraphy of chironomid composition in the training set lakes. Only taxa present in two samples or more are represented. The lakes have been ordered by WMM (cold to warm). The zones have been arbitrary created by WMM. The x-axes are in percentage, except for the number of head capsules.

assemblages were dominated by Tanytarsini 1A, *Riethia*, Tanytarsini 1B and *Chironomus*. During the ACR/YD (14500–11,000 cal yr BP), *Riethia* gradually decreased and disappeared after the YD. Tanytarsini 1A also decreased but increased again after 10,700 cal yr BP. Many taxa appeared during the ACR and disappeared afterwards such as *Gymnotetia*, *Djalmabattista*, *Paracladopelma*, *Parakiefferiella fennica*, *Cladotanytarsus* and *Apedilum*. Other taxa, such as *Macropelopia*, *Harrisius* and *Labrundinia* have a peak during the ACR. Most of the dominant taxa during the ACR decreased during the YD, except *Chironomus*, *Smitia*/*Parasmitia* and other semi-terrestrial taxa that include, *Pseudosmittia*, *Stictocladius* and *Bryophaenocladius*. When the chironomid assemblages of the Huelmo samples were added passively into a CCA of the training set lakes, all samples were located within the training set assemblages (Fig. 7). This result suggests that the developed transfer function could be applied to the Huelmo samples.

4.5. Paleotemperature reconstruction at Huelmo

The three models were used to reconstruct WMM at Huelmo. The model with >15 hc showed the highest variability, followed by the model with all lakes and the model with >30 hc (Fig. 8). Since the model statistics were slightly better for the model with >15 hc, a three-point running mean was made using this model. The chironomid-inferred WMM between 19,000 and 16,000 cal yr BP were colder than the mean chironomid-inferred WMM of the whole period (19,000–10,000 cal yr BP). A cold interval (–1 °C) was inferred at ca. 15,700 cal yr BP but only in one sample. The temperatures oscillated around the average until ca. 14,500 cal yr BP. They were warmer than the average between 14,500 and 13,000 cal yr BP. Another cold interval (–1.4 °C) was inferred in three samples between 13,200 and 13,000 cal yr BP. The chironomid-inferred temperatures were above average until cal yr BP when they started to decrease. Two cold intervals were inferred at ca. 12,600 cal yr BP (two samples) and ca. 11,700 cal yr BP (two samples). The chironomid-inferred WMM were constantly warmer than the average between 11,600 and 10,000 cal yr BP.

5. Discussion

5.1. Chironomids, temperature and other environmental variables

Since the early work of Walker et al. (1995), temperature has been shown to be one of the most important variables affecting the distribution of chironomids in lakes distributed along a large temperature gradient (e.g. Lotter et al., 1997; Olander et al., 1999; Brooks and Birks, 2001; Larocque et al., 2001, 2006; Massferro and Larocque, 2013). Other environmental variables influencing chironomids are nutrients (Lotter et al., 1998), depth (Korhola et al., 2000), conductivity (Larocque et al., 2006), oxygen (Quinlan and Smol, 2001b), pH (Rees and Cwynar, 2010) and macrophytes (Langdon et al., 2010). Except for oxygen and macrophytes, all the other variables were measured in the north Patagonian training set and temperature has been identified, again, as the most significant variable explaining the distribution

Table 2 Model statistics.

	WA-PLS	Lakes	Nb species	Components	r ² jack	Max. bias	RMSEP	r ²	RMSE
All	46	49	1		0.51	2.68	1.82	0.93	0.67
>30 hc	34	49	3		0.47	2.26	1.76	0.95	0.55
			1						
>15 hc	41	49	2		0.56	2.07	1.69	0.93	0.63
			3						
			3						

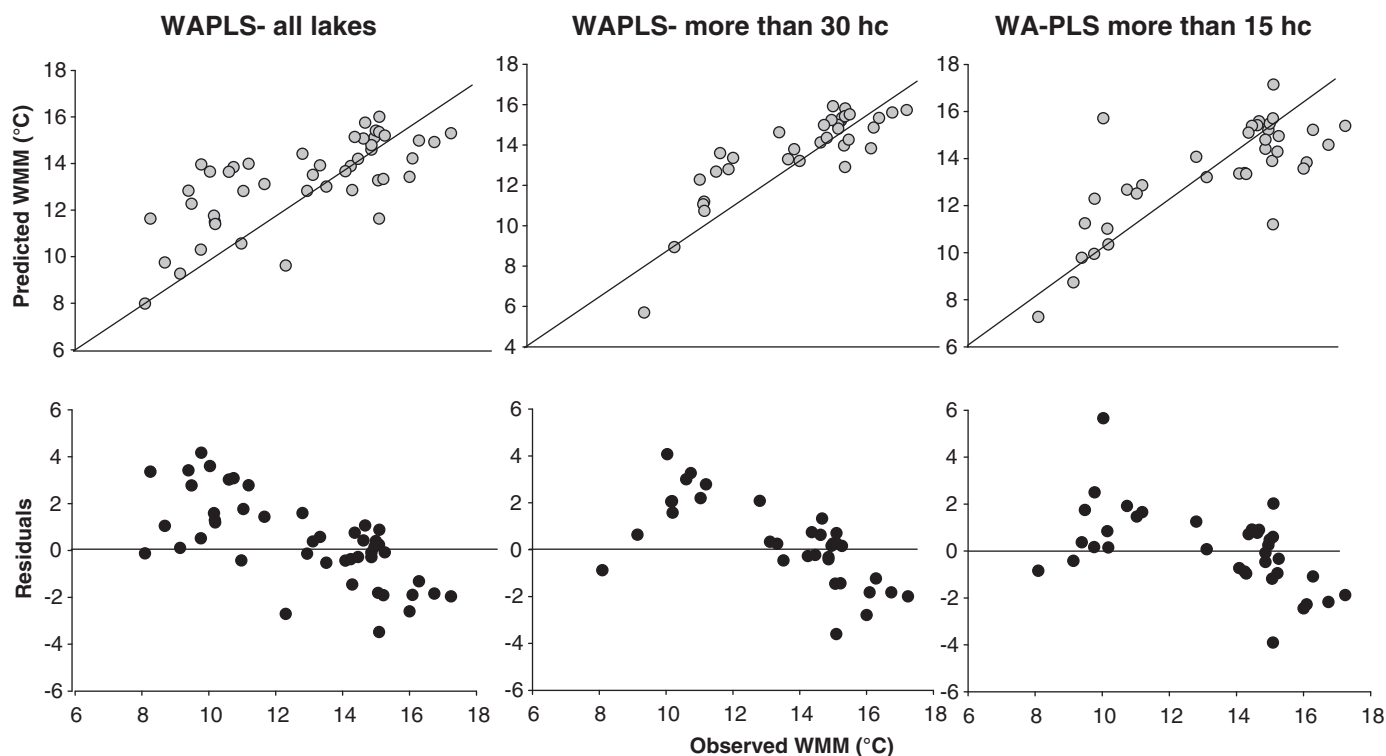


Fig. 5. Presentation of the three WA-PLS models: with all lakes, with lakes having at least 30 head capsules (more than 30 hc) and with lakes having more than 15 head capsules (more than 15 hc). In the upper graphs, the diagonal line represents the 1:1 relationship.

and abundance of chironomids in northern Patagonia, followed by conductivity and secchi depth. Summer temperature directly affects the rate of chironomid egg and larval development and in these ultra/oligotrophic lakes is the most important variable having direct ecological effect on chironomid assemblages. Conductivity and secchi depth (transparency) are both linked to the amount of suspended material coming from melting water or from the landscape. Conductivity is commonly higher in lakes located closer to centers of human population than in more remote lakes. In high elevation lakes connected to a glacier such as some of the lakes in this study, secchi depth was low and conductivity was high due to the entry of high amounts of suspended material.

5.2. Taxonomic notes of northern Patagonian chironomids

Smittia was identified as a cold indicator due to its abundance in lakes below 10 °C, even though it was present in very low percentages (less than 10%) in lakes up to WMM of 12 °C. In the southern Patagonia training set (Massafarro and Laroque, 2013) and in the eastern-North America training set (Laroque, 2008) *Smittia* was also a cold indicator.

In this study, most of the Tanytarsini dominated low elevation sites with WMM > 14 °C, except *Tanytarsini* sp C which was restricted to lakes in the middle temperature range (12–14 °C). *Tanytarsini* sp C is also a cold indicator, having a temperature optimum similar to *Micropsectra* in the northern Hemisphere and *Tanytarsus funebris* type C in New Zealand (Brooks and Birks, 2001; Laroque, 2008, Vandergoes et al., 2007). Despite the resemblances, Patagonian Tanytarsini (Massafarro et al., 2013) in general revealed warmer optima than those from the northern Hemisphere. For instance, *Tanytarsini* 1B has similar morphological features than *Tanytarsus lugens* but it was found in warm low altitudinal lakes. In addition, other taxa such as *Micropsectra* or *Corynocera* commonly found in cold northern lakes, are absent in South America.

Chironomus is a warm indicator present in high concentrations in eutrophic, lowland lakes from the northern Hemisphere. Recent studies from the southern Hemisphere revealed that *Chironomus* can

be abundant at both cold high-altitude oligotrophic lakes and warm low-altitude eutrophic lakes (Woodward and Shulmeister, 2006a). In southern Patagonia, Massafarro et al. (2009, 2010) showed the highest abundance of *Chironomus* in high-elevation sites (above 1000 m) with low water temperatures. Similar results were found in New Zealand by Dieffenbacher-Krall et al. (2007), whereas Woodward and Shulmeister (2006b) found both warm- and cold-adapted *Chironomus* species in New Zealand. In this study, this taxon dominates the middle to upper temperature range (12–16 °C) below the treeline (ca. 1000 m a.s.l.). We conclude that many species of *Chironomus* must be present in our Patagonian dataset.

Riethia is a genus endemic of the southern Hemisphere. In this study, it appeared in lakes located in a range of middle to low temperatures (12 to 10 °C). Dimitriadis and Cranston (2001) developed a quantitative paleoenvironmental inference model for tropical Australia in which they showed *Riethia* as a cold-stenothermic taxon. Either, in Tasmania, *Riethia* was found in higher abundances at elevations above 600 m a.s.l. and its distribution showed a significant relationship with cold temperatures (Rees et al., 2008).

Further studies to resolve both taxonomic and ecological aspects of these taxa at mid-latitudes of the Southern Hemisphere are required.

5.3. Cooling at the Late Glacial/Holocene transition at mid latitudes of the southern Hemisphere

There is no consensus as to whether the Northern and Southern Hemispheres respond synchronously or out-of-phase to climate forcing mechanisms (Schaefer et al., 2006; Kaplan et al., 2008; Barker et al., 2010). Denton et al. (2010) discussed the complex North–South connections during the Last Glacial Termination considering that different mechanisms explained climate divergences between both hemispheres involving the oceanic bipolar see-saw, the position and intensity of the SWW, and the global reorganization of atmospheric circulation during the Last Termination. Recent paleoclimate records from southern latitudes indicate a cold reversal at the end of the last glacial period

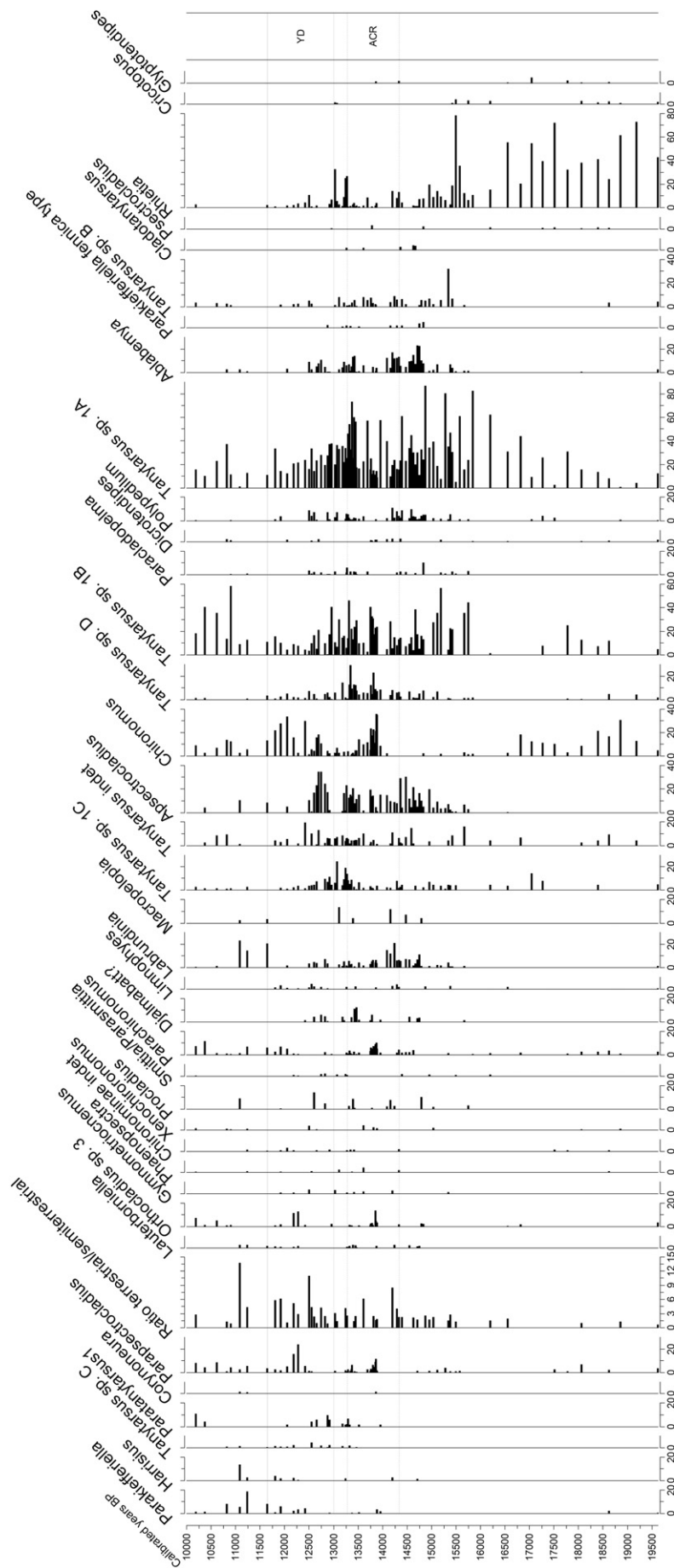


Fig. 6. Stratigraphy of chironomid composition through time in Huelmo. Only taxa present in two samples or more are shown. The x-axes are in percentage, except for the number of head capsules.

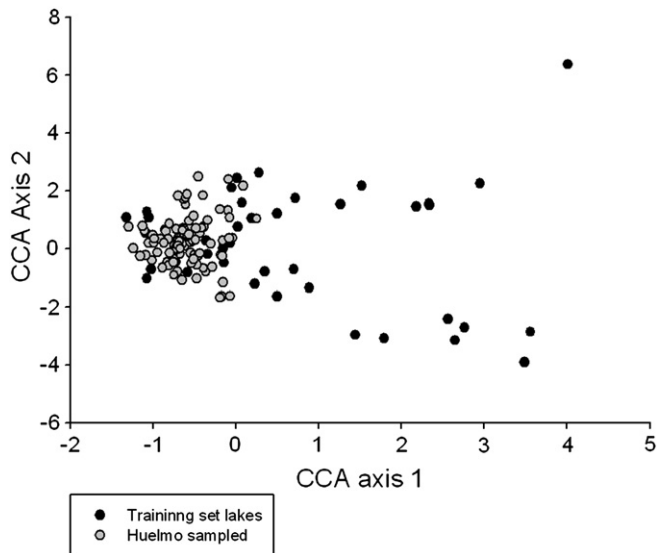


Fig. 7. Distribution of Huelmo's samples (gray circles) within a CCA of the training set lakes (black circles).

coincident with the Antarctic Cold Reversal (ACR) rather than with the Younger Dryas (YD) cooling (Newnham and Lowe, 2000; Vandergoes et al., 2008). In southern South America, a study by Hajdas et al. (2003) characterized a distinct cold reversal on both sides of the Andean cordillera: the Huelmo–Mascardi Cold Reversal (HMCR), which occurred between 13,200 and 12,600 cal yr BP, encompassing the timing of the Gerzensee/Killarney oscillation, and the YD in the Northern Hemisphere. Following this study, Bertrand et al. (2008a) and Boes and Fagel (2008), using a multiproxy paleoreconstruction from Lago Puyehue (~41° S), suggested the existence and timing of the HMCR in the region. At the same latitude but on the western side of the Andes in Lago Mascardi, geochemical proxies and pollen records indicated a re-advance of El Manso glacier and a change in the vegetation in the Rio Manso superior valley between 13,000 and 11,500 cal yr BP, which is consistent with the HMCR event (Bianchi & Ariztegui, 2012).

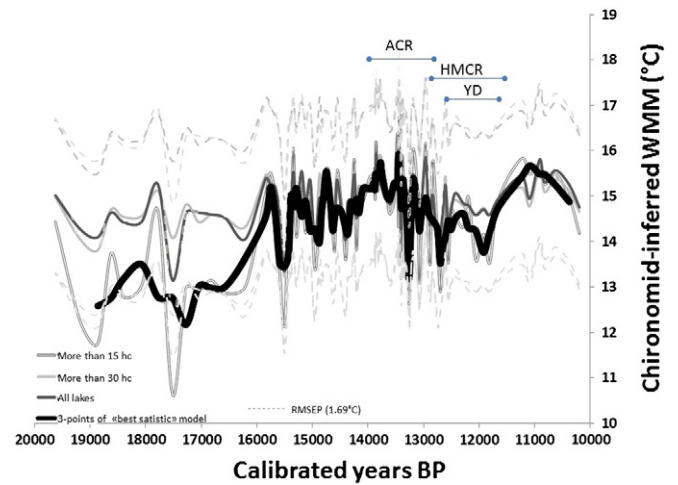


Fig. 8. Huelmo reconstruction showing the three WAPLS models: including all the lakes (plain black line), including lakes with >30 head capsules (plain gray line) and including lakes with >15 head capsules (dotted line). A three-point running mean of the best statistical model (WAPLS > 15 hc) is shown in thick black line. Sample specific errors were included in the diagram. Younger Dryas (YD), the Huelmo–Mascardi Cold Reversal (HMCR) and the Antarctic Cold Reversal (ACR) are also shown.

In a previous pollen and chironomid study at Huelmo, Massaferrero et al. (2009) identified a climate signal similar to the YD but of broader amplitude. This cooling showed initial cold-humid conditions (13,200–12,600 cal yr BP) dominated by cold stenothermic chironomid and pollen taxa which was associated to the HMCR and, a successive shift to relatively drier conditions (between 12,600 and 11,000 cal yr BP) evidenced by fire activity, pollen species associated with disturbance, and littoral chironomids (indicators of water level changes).

Our Huelmo quantitative reconstruction suggests deglacial warming up to ca. 15,000 cal yr BP followed by more stable conditions until about 13,200 cal yr BP when a cold phase initiated and persisted until 11,500 cal yr BP. The cool interval shown in our quantitative reconstruction of the Huelmo record broadly coincides with the ACR recorded in Antarctic ice cores (Pedro et al., 2011). In our reconstruction, temperatures oscillated around the average from 15,500 cal yr BP until ca.

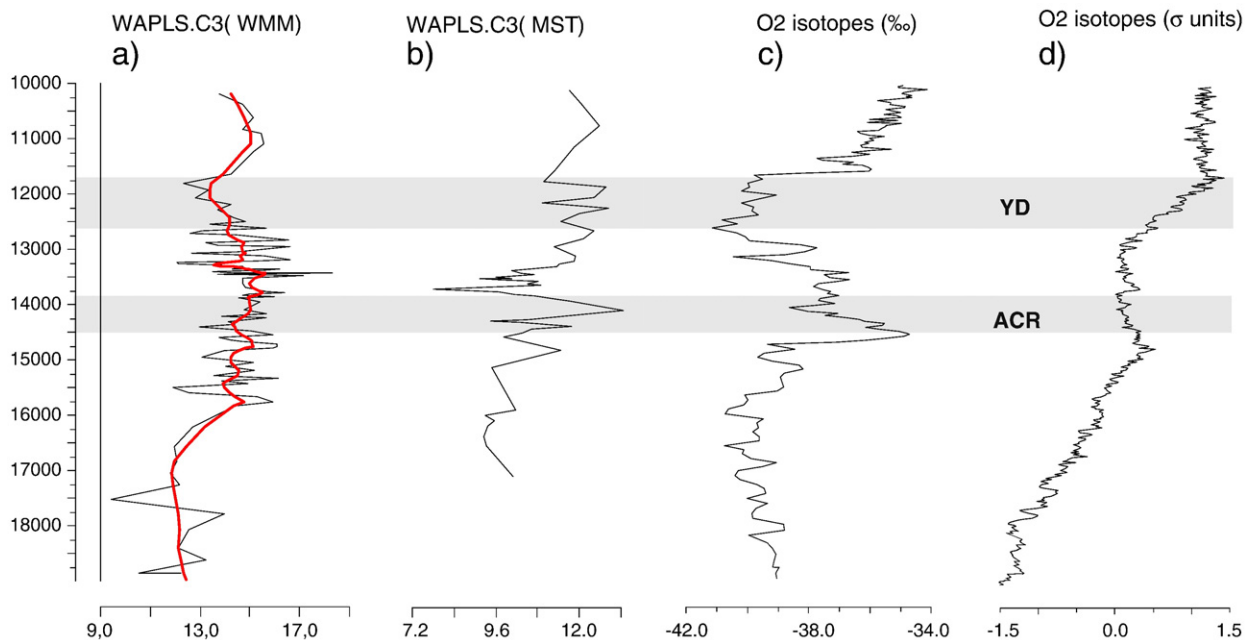


Fig. 9. (a) WMM Huelmo reconstruction with LOWESS smooth line (0.1) in gray to highlight the major trends compared to (b) Boundary Stream Tarn (New Zealand) MST (mean summer temperature) reconstruction, (c) Greenland GISP2 oxygen isotope record (Alley, 2000) and (d) Antarctic composite oxygen isotope record (Pedro et al., 2011).

14,500 cal yr BP. Cold spells were recorded in Huelmo reconstruction at 13,200 to 13,000 cal yr BP and 12,600 to 11,500 cal yr BP. These reversals may be associated with the HMCR and the YD. The termination of the cooling coincides with the onset of the Holocene (Fig. 9).

Our findings support evidence suggesting a fast-acting inter-hemispheric coupling of climate mechanisms, including bipolar atmospheric and/or bipolar ocean teleconnections rather than a bipolar see-saw (Lamy et al., 2004; Denton et al., 2010; Pedro et al., 2011).

In New Zealand, a quantitative chironomid reconstruction at Boundary Stream Tarn (Vandergoes et al., 2007) indicates cooling coincident with the ACR signal and no clear evidence that this climate reversal persisted into the YD chron (Fig. 9). A chironomid based temperature reconstruction from Tasmania (Rees et al., 2008) does not provide clear evidence of an ACR or YD cooling.

6. Conclusions

Quantitative temperature reconstructions from the Southern Hemisphere are extremely valuable to clarify climate relationships between both hemispheres. This investigation shows that chironomid distribution and abundance in the 46 Patagonian lakes surveyed were strongly influenced by WMM. Furthermore, the good performance statistics of a chironomid-based WMM inference model and the fact that summer temperature has a direct impact through life history effects on chironomid distribution and abundance indicate that midges are an appropriate proxy for modeling the temperature of northern Patagonia. The chironomid temperature reconstruction presented here is the first such in the area of northern Patagonia and provides robust estimates of summer temperature during the Late Glacial/Holocene transition at Huelmo site located in the Chilean Lake District of Patagonia. The chironomid reconstruction is consistent with other lines of evidence that suggest Late Glacial climate reversal at the time of the ACR/YD.

Acknowledgments

We thank Sarah Gilchrist for collecting some of the samples and for preliminary chironomid analysis. JM acknowledges G. Denton and COMER Science Foundation for providing financial support and M. Colombres for lab assistance.

References

Alley, R.B., 2000. The Younger Dryas cold interval as view from Central Greenland. *Quat. Sci. Rev.* 19, 213–226.

Araneda, A., 2013. Developing a quantitative reconstruction of temperature in Southern Chile, for the last millennium based on midge assemblages. 12th International Workshop of Subfossil Chironomidae, New Forest, UK 10–13 June, 2013.

Ariztegui, D., Bianchi, M., Massafiero, J., Lafargue, E., Niessen, F., 1997. Interhemispheric synchrony of late-glacial climatic instability as recorded in proglacial Lake Mascardi, Argentina. *J. Quat. Sci.* 12, 333–338.

Balseiro, E., Quimaliños, C., Modenutti, B., 2004. Grazing impact on autotrophic picoplankton in two south Andean lakes (Patagonia, Argentina) with different light:nutrient ratios. *Rev. Chil. Hist. Nat.* 77, 73–85.

Barker, S., Knorr, G., Vautraviers, M.J., Diz, P., Skinner, L.C., 2010. Extreme deepening of the 15 Atlantic circulation during deglaciation. *Nat. Geosci.* 3, 567–571.

Bertrand, S., Charlet, F., Charlier, B., Renson, V., Fagel, N., 2008a. Climate variability of southern Chile since the Last Glacial Maximum: a continuous sedimentological record from Lago Puyehue (408 S). *J. Paleolimnol.* 39, 179–195. <http://dx.doi.org/10.1007/s10933-007-9117-y>.

Bertrand, S., Charlet, F., Charlier, B., Renson, V., Fagel, N., 2008b. Climate variability of southern Chile since the Last Glacial Maximum: a continuous sedimentological record from Lago Puyehue (408S). *J. Paleolimnol.* 39 (2), 219–235.

Bianchi, M.M., Ariztegui, D., 2012. Vegetation history of the Rio Manso superior catchment area, northern Patagonia (Argentina), since the Last deglaciation. *The Holocene* 22 (11), 1283–1295.

Birks, H.J.B., 1998. D.G. Frey & E.S. Deevey Review #1. Numerical tools in palaeolimnology – progress, potentialities, and problems. *J. Paleolimnol.* 20, 307–332.

Boes, X., Fagel, N., 2008. Relationships between southern Chilean varved lake sediments, precipitation and ENSO for the last 600 years. *J. Paleolimnol.* 39, 219–235. <http://dx.doi.org/10.1007/s10933-007-9118-x>.

Borcard, D., Legendre, P., Drapeau, P., 1992. Partialling out the spatial component of ecological variation. *Ecology* 73, 1045–1055.

Brodersen, K.P., Lindegaard, C., 1999. Classification, assessment and trophic reconstruction of Danish lakes using chironomids. *Freshw. Biol.* 42, 143–157.

Brooks, S.J., Birks, H.J.B., 2001. Chironomid-inferred air temperatures from late glacial and Holocene sites in northwest Europe: progress and problems. *Quat. Sci. Rev.* 20, 1723–1741.

Callieri, C., Modenutti, B., Quimaliños, C., Bertoni, R., Balseiro, E., 2007. Production and biomass of picophytoplankton and larger autotrophs in Andean ultraoligotrophic lakes: differences in light harvesting efficiency in deep layers. *Aquat. Ecol.* 41, 511–523.

Cranston, P.S., 2000. Electronic Guide to the Chironomidae of Australia. <http://entomology.ucdavis.edu/chiropage/index.html>.

Denton, G.H., Hendy, C.H., 1994. Younger Dryas age advance of Franz Josef Glacier in the Southern Alps of New Zealand. *Science* 264 (5164), 1434–1437.

Denton, G.H., Anderson, R.F., Toggweiler, J.R., Edwards, R.L., Schaefer, J.M., Putnam, A.E., 2010. The last glacial termination. *Science* 328, 1652–1656.

Diaz, M., Pedrozo, F., Reynolds, C., Temporetti, P., 2007. Chemical composition and the nitrogen-regulated trophic state of Patagonian lakes. *Limnologia* 37, 17–27.

Dieffenbacher-Krall, A.C., Vandergoes, M.J., Denton, G.H., 2007. An inference model for mean summer air temperatures in the Southern Alps, New Zealand using subfossil chironomids. *Quat. Sci. Rev.* 26, 2487–2504.

Dimitriadis, S., Cranston, P.S., 2001. An Australian Holocene climate reconstruction using Chironomidae from a tropical volcanic maar lake. *Palaeogeogr. Palaeoclimatol. Palaeoecol.* 176, 109–131.

Eggermont, H., Heiri, O., 2012. The chironomid–temperature relationship: expression in nature and palaeoenvironmental implications. *Biol. Rev.* 87, 430–456.

Garreaud, R., Vuille, M., Compagnucci, R., Marengo, J., 2009. Present-day South American climate. *Palaeogeogr. Palaeoclimatol. Palaeoecol.* 281, 180–195.

Hajdas, I., Bonani, G., Moreno, P.L., Ariztegui, D., 2003. Precise radiocarbon dating of late glacial cooling in mid-latitude South America. *Quat. Res.* 59, 70–78.

Heiri, O., Lotter, A.F., 2001. Effect of low count sums on quantitative environmental reconstructions: an example using subfossil chironomids. *J. Paleolimnol.* 26, 343–350.

Heusser, C.J., 1999. Human forcing of vegetation change since the last ice age in southern Chile and Argentina. *Bamberger Geographische Schriften* 19, 211–231.

Heusser, C.J., Lowell, T.V., Heusser, L.E., et al., 1996. Full-glacial late-glacial paleoclimate of the southern Andes. Evidence from pollen, beetle, and glacial records. *J. Quat. Sci.* 11, 173–184.

Hill, M.O., Gauch, H.G., 1980. Detrended correspondence analysis: an improved ordination technique. *Vegetatio* 42, 47–68.

Jouzel, J., Vimeux, F., Caillon, N., Delaygue, G., Hoffmann, G., Masson-Delmotte, V., Parrenin, F., 2003. Magnitude of isotope/temperature scaling for interpretation of central Antarctic ice cores. *J. Geophys. Res.* 108, 4361.

Juggins, S., 2007. C2 Version 1.5 User Guide. Software for Ecological and Palaeoecological Data Analysis and Visualisation University of Newcastle, Newcastle-upon-Tyne.

Kaplan, M.R., Fogwill, C.J., Sugden, D.E., Hulton, N.R.J., Kubik, P.W., Freeman, S.P.H.T., 2008. Southern Patagonian and Southern Ocean climate during the last glacial period. *Quat. Sci. Rev.* 27, 284–294.

Killian, R., Lamy, F., 2012. A review of Glacial and Holocene paleoclimate records from southernmost Patagonia (49–55 S). *Quat. Sci. Rev.* 53, 1–23.

Korhola, A., Olander, H., Blom, T., 2000. Cladoceran and chironomid assemblages as quantitative indicators of water depth in subarctic Fennoscandian lakes. *J. Paleolimnol.* 24, 43–54.

Lamy, F., Kaiser, J., Ninnemann, U., Hebbeln, D., Arz, H.W., Stoner, J., 2004. Antarctic timing of surface water changes off Chile and Patagonian ice sheet response. *Science* 304, 1959–1962.

Langdon, P.G., Ruiz, Z., Wynne, S., Sayer, C.D., Davidson, T.A., 2010. Ecological influences on larval chironomid communities in shallow lakes: implications for palaeolimnological interpretations. *Freshw. Biol.* 55 (3), 531–545.

Larocque, I., 2008. Nouvelle fonction de transfert pour reconstruire la température à l'aide des chironomides pré-servés dans les sédiments lacustres. INRS Rapport de Recherche R1032, ISBN 978-2-89146-587-8.

Larocque, I., Hall, R.L., Grahn, E., 2001. Chironomids as indicators of climatic and environmental change: a 100-lake training set from a subarctic region of northern Sweden (Lapland). *J. Paleolimnol.* 26, 307–322.

Larocque, I., Pienitz, R., Rolland, N., 2006. Factors influencing the distribution of chironomids in lakes distributed along a latitudinal gradient in northwestern Québec, Canada. *Can. J. Fish. Aquat. Sci.* 63, 1286–1297.

Larocque, I., Grosjean, M., Heiri, O., Bigler, C., Blass, A., 2009. Comparison between chironomid-inferred July temperatures and meteorological data AD 1850–2001 from varved Lake Silvaplana, Switzerland. *J. Paleolimnol.* 41, 329–342.

Lotter, A.F., Birks, H.J.B., Hofmann, W., Marchetto, A., 1997. Modern diatom, cladocera, chironomid, and chrysophyte cyst assemblages as quantitative indicators for the reconstruction of past environmental conditions in the Alps. I: climate. *J. Paleolimnol.* 18, 395–420.

Lotter, A.F., Birks, H.J.B., Hofmann, W., Marchetto, A., 1998. Modern diatom, cladocera, chironomid, and chrysophyte cyst assemblages as quantitative indicators for the reconstruction of past environmental conditions in the Alps. II. Nutrients. *J. Paleolimnol.* 19, 443–463.

Massafiero, J., Brooks, S.J., 2002. Response of chironomids to Late Quaternary environmental change in the Taitao Peninsula, southern Chile. *J. Quat. Sci.* 17, 101–111.

Massafiero, J., Larocque, I., 2013. Using a newly developed chironomid transfer function for reconstructing mean annual temperature at Lake Potrok Aike, Patagonia, Argentina. *Ecol. Indic.* 24, 201–210.

Massafiero, J., Vandergoes, M., 2013. Postglacial southern hemisphere. In: Elias, S.A. (Ed.), *The Encyclopedia of Quaternary Science*, vol. 1. Elsevier, Amsterdam, pp. 398–405.

- Massafarro, J., Moreno, P.I., Denton, G.H., Vandergoes, M., Dieffenbacher-Krall, A., 2009. Chironomid and pollen evidence for climate fluctuations during the Last Glacial Termination in NW Patagonia. *Quat. Sci. Rev.* 28, 517–525.
- Massafarro, J., Manca, M., Sylvestre, F., Ariztegui, D., 2010. Late Glacial/early Holocene reconstruction from Lake Mascardi (Patagonia, Argentina) using a multibioproxy approach. II International Symposium PAGES “Reconstructing Climate Variations in South America and the Antarctic Peninsula over the last 2000 years”, October 27–30.
- Massafarro, J., Ortega, C., Fuentes, C., Araneda, A., 2013. Clave para la identificación de Tanytarsini (INSECTA: Diptera: Chironomidae: Chironominae) cuaternarios de la Patagonia. *Ameghiniana* 50 (3), 319–334.
- McGlone, M., Turney, C., Wilmshurst, J., 2004. Late-glacial and Holocene vegetation and climatic history of the Cass Basin, central South Island, New Zealand. *Quat. Res.* 62, 267–279.
- Moreno, P.I., 1997. Vegetation and climate near Lago Llanquihue in the Chilean lake district between 20,200 and 9,500 14C yr BP. *J. Quat. Sci.* 12, 485–500.
- Moreno, P.I., 2004. Millennial-scale climate variability in northwest Patagonia over the last 15000 yr. *J. Quat. Sci.* 19 (1), 35–47.
- Moreno, P.I., Leon, A.L., 2003. Abrupt vegetation changes during the last glacial to Holocene transition in mid-latitude South America. *J. Quat. Sci.* 18, 787–800.
- Moreno, P.I., Jacobson, J.L., Lowell, T.V., Denton, G., 2001. Interhemispheric climate links revealed by a late-glacial cooling episode in southern Chile. *Nature* 409, 804–808.
- Moreno, P.I., Kaplan, M.R., François, J.P., Villa-Martínez, R., Moy, C., Stern, C.R., Kubik, P., 2009. Renewed glacial activity during the Antarctic Cold Reversal and persistence of cold conditions until 11.5 ka in southwestern Patagonia. *Geology* 37, 375–378.
- New, M., Lister, D., Hulme, M., Makin, I., 2002. A high-resolution data set of surface climate over global land areas. *Clim. Res.* 21, 1–25.
- Newnham, R.M., Lowe, D.J., 2000. Fine-resolution pollen record of Late Glacial climate reversal from New Zealand. *Geology* 28, 759–762.
- Newnham, R., Eden, D., Lowe, D., Hendy, C., 2003. Rerewhakaaitu Tephra, a land–sea marker for the Last Termination in New Zealand, with implications for global climate change. *Quat. Sci. Rev.* 22, 289–308.
- Olander, H., Birks, H.J.B., Korhola, A., Blom, T., 1999. An expanded calibration model for inferring lakewater and air temperatures from fossil chironomid assemblages in northern Fennoscandia. *The Holocene* 9, 279–294.
- Quinlan, R., Smol, J.P., 2001a. Setting minimum head capsule abundance chironomid-based inference models. *J. Paleolimnol.* 26, 327–342.
- Quinlan, R., Smol, J.P., 2001b. Chironomid-based inference models for estimating end-of-summer hypolimnetic oxygen from south-central Ontario shield lakes. *Freshw. Biol.* 46, 1529–1555.
- Rees, A.B.H., Cwynar, L.C., 2010. A test of Tyler’s Line — response of chironomids to a pH gradient in Tasmania and their potential as a proxy to infer past changes in pH. *Freshw. Biol.* 55, 2521–2540.
- Rees, A.B.H., Cwynar, L., Cranston, P.S., 2008. Midges (Chironomidae, Ceratopogonidae, Chaoboridae) as a temperature proxy: a training set from Tasmania, Australia. *J. Paleolimnol.* 40, 1159–1178.
- Rojas, M., Moreno, P.I., Kageyama, M., Crucifí x, M., Hewitt, C., Abe-Ouchi, A., Ohgaito, R., Brady, E.C., Hope, P., 2009. The southern westerlies during the last glacial maximum in PMIP2 simulations. *Clim. Dyn.* 32, 525–548.
- Rosén, P., Hall, R., Korsman, T., Renberg, I., 2000. Diatom transfer — functions for quantifying past air temperature, pH and total organic carbon concentration from lakes in northern Sweden. *J. Paleolimnol.* 24, 109–123.
- Rossaro, B., 1991. Chironomids and water temperature. *Aquat. Insects* 13, 87–98.
- Schaefer, J.M., Denton, G.H., Barrell, D.J.A., Ivy-Ochs, S., Kubic, P.W., Anderson, B.G., Phillips, F.M., Lowell, T.V., Schluchter, C., 2006. Mid-latitude moraines reveal near-synchronous interhemispheric termination of the Last Glacial Maximum. *Science* 312, 1510–1513.
- Self, A.E., Brooks, S.J., Birks, H.J.B., Nazarova, L., Porinchu, D., Odland, A., Yang, H., Jones, V.J., 2011. The distribution and abundance of chironomids in high-latitude Eurasian lakes with respect to temperature and continentality: development and application of new chironomid-based climate-inference models in northern Russia. *Quat. Sci. Rev.* 30, 1122–1141.
- Stuiver, M., Reimer, P.J., Reimer, R.W., 2005. CALIB 5.0. WWW Program and Documentation.
- ter Braak, C.J.F., 1990. Update Notes: CANOCO version 3.10. Agricultural Mathematics Group, Wageningen.
- ter Braak, C.J.F., Juggins, S., 1993. Weighted averaging partial least squares regression (WA-PLS): an improved method for reconstructing environmental variables from species assemblages. *Hydrobiologia* 269 (270), 485–502.
- ter Braak, C.J.F., Smilauer, P., 1998. CANOCO Reference Manual and User’s Guide to CANOCO for Windows: Software for Canonical Community Ordination (version 4). Microcomputer Power, Ithaca, NY, USA (352 pp.).
- ter Braak, C.J.F., Verdonschot, P.F.M., 1995. Canonical correspondence analysis and related multivariate methods in aquatic ecology. *Aquat. Sci.* 57, 255–289.
- Turney, C.S.M., McGlone, M.S., Wilmshurst, J.M., 2003. Asynchronous climate change between New Zealand and the North Atlantic during the last deglaciation. *Geology* 31, 223–226.
- Pedro, van Ommen, T.D., Rasmussen, S.O., Morgan, V.I., Chappellaz, J., Moy, A.D., Masson-Delmotte, V., Delmotte, M., 2011. The last deglaciation: timing the bipolar seesaw. *Clim. Past Discuss.* 7, 397–430. <http://dx.doi.org/10.5194/cpd-7-397-2011>.
- Vandergoes, M.J., Dieffenbacher-Krall, A.C., Newnham, R.M., Denton, G.H., Blaauw, M., 2007. Cooling and changing seasonality in the Southern Alps, New Zealand during the Antarctic Cold Reversal. *Quat. Sci. Rev.* 27, 589–601.
- Vandergoes, M.J., Dieffenbacher-Krall, A.C., Newnham, R.M., Denton, G.H., Blaauw, M., 2008. Cooling and changing seasonality in the southern Alps, New Zealand during the Antarctic cold reversal. *Quat. Sci. Rev.* 27, 589–601.
- Walker, I., Smol, J., Engstrom, D., Birks, H.J.B., 1991. An assessment of Chironomidae as quantitative indicators of past climatic change. *Can. J. Fish. Aquat. Sci.* 48, 975–987.
- Walker, I.R., Wilson, S.E., Smol, J.P., 1995. Chironomidae (Diptera): quantitative palaeosalinity indicators for lakes of western Canada. *Can. J. Fish. Aquat. Sci.* 52, 950–960.
- Whitlock, C., Bianchi, M.M., Bartlein, P.J., Markgraf, V., Marlon, J., Walsh, M., McCoy, N., 2006. Postglacial vegetation, climate, and fire history along the east side of the Andes (lat 41–42.5 degrees S), Argentina. *Quat. Res.* 66, 187–201.
- Wiederholm, T. (Ed.), 1983. Chironomidae of the Holarctic Region. Keys and Diagnoses. Part 1—Larvae. Entomol. Scandinav., Supplement 19 (457 pp.).
- Woodward, C.A., Shulmeister, J., 2006a. New Zealand chironomids as proxies for human-induced and natural environmental change: transfer functions for temperature and lake production (chlorophyll a). *J. Paleolimnol.* 36 (4), 407–429.
- Woodward, C.A., Shulmeister, J., 2006b. New Zealand chironomids as proxies for human-induced and natural change: Transfer functions for temperature and lake production (chlorophyll a). *J. Paleolimnol.* 36 (4), 381–501.
- Woodward, C.A., Shulmeister, J., 2007. Chironomid-based reconstructions of summer air temperature from lake deposits in Lyndon Stream, New Zealand spanning the MIS 3/2 transition. *Quat. Sci. Rev.* 26, 142–154.